3-D topology optimization of single-pole-type head by using design sensitivity analysis

Yoshifumi Okamoto
Okayama University

Koji Akiyama
Okayama University

Norio Takahashi
Okayama University

3-D Topology Optimization of Single-Pole-Type Head by Using Design Sensitivity Analysis

Y. Okamoto, K. Akiyama, and N. Takahashi, *Fellow, IEEE*

Department of Electrical and Electronic Engineering, Okayama University, Okayama 700-8530, Japan

It is necessary to develop a write head having a large recording field and small stray field in adjacent tracks and adjacent bits in perpendicular magnetic recording systems. In this paper, a practical three-dimensional topology optimization technique combined with the edge-based finite-element method is proposed. A technique for obtaining a smooth topology is also shown. The optimization of single-pole-type head having a magnetic shield is performed by using the topology optimization technique so that the leakage flux in the adjacent bit can be reduced. A useful shape of the magnetic shield obtained by the proposed technique is illustrated.

Index Terms—**ON/OFF method, sensitivity analysis, single-pole-type-head, three-dimensional (3-D) topology optimization.**

I. Introduction

THE perpendicular magnetic recording system is considered as an important technique for the high-density magnetic recording system reaching 1 Tb/in^2. As a result of the dramatic increment of the recording density, the erasing of bits due to the stray field becomes remarkable. With this background, the purpose of our research is the optimal design of a writing head having a magnetic shield by using the topology optimization technique (ON/OFF method [1], [2]).

The topology optimization is an attractive method for designers of magnetic devices because an initial conceptual design can be obtained. However, the report of the three-dimensional (3-D) topology optimization of magnetic devices is few [3]. Then, we propose the 3-D topology optimization technique combined with the edge-based finite-element method (FEM). The algorithm of the ON/OFF method is shown. A new technique called the "topology smoother" for avoiding an uneven region is developed. In the 3-D optimization problem, a numerous iteration of the FEM calculation in consideration of the nonlinear magnetic characteristic is needed. Then, in order to reduce the central processing unit (CPU) time, the Newton–Raphson method, using the line-search technique, is introduced [4]. The 3-D topology optimization of the single-pole-type (SPT) head is performed using the combinatorial method of the ON/OFF method and CPU time reduction method. The effect of the weighting coefficient of the objective function is examined.

II. Optimization Method

A. Design Sensitivity Analysis

In the optimization method proposed in this paper, the existence of the magnetic material in the design domain is determined using a sensitivity $\mathrm{d}W/\mathrm{d}\nu_i$ (the derivative of the objective function W with respect to the reluctivity ν_i). The adjoint variable method [5] taking into account the nonlinear magnetic property is applied as a sensitivity analysis method. The derivative of the objective function W with respect to the reluctivity ν_i in an element i is given as

$$\frac{\mathrm{d}W}{\mathrm{d}\nu_i} = \frac{\partial W}{\partial \nu_i} + \left(\frac{\partial W}{\partial \boldsymbol{A}}\right)^T \frac{\partial \boldsymbol{A}}{\partial \nu_i} \tag{1}$$

where $\boldsymbol{A}$ is the magnetic vector potential assigned to edge in finite elements. The equation for FEM is given as

$$\boldsymbol{H}A = \boldsymbol{G} \tag{2}$$

where $\boldsymbol{H}$ is the coefficient matrix and $\boldsymbol{G}$ is the right-hand-side vector. If the residual vector $\boldsymbol{r}$ is used, (2) is given as

$$\boldsymbol{r} = \boldsymbol{H}A - \boldsymbol{G}. \tag{3}$$

The derivative of the residual vector $\boldsymbol{r}$ with respect to the reluctivity ν_i in an element i is given as

$$\frac{\mathrm{d}\boldsymbol{r}}{\mathrm{d}\nu_i} = \frac{\partial \boldsymbol{r}}{\partial \nu_i} + \frac{\partial \boldsymbol{r}}{\partial \boldsymbol{A}}\frac{\partial \boldsymbol{A}}{\partial \nu_i}. \tag{4}$$

Substituting (3) into (4), the first term of the right-hand side of (4) is given as

$$\frac{\partial \boldsymbol{r}}{\partial \nu_i} = \frac{\partial \boldsymbol{H}}{\partial \nu_i}\boldsymbol{A} - \frac{\partial \boldsymbol{G}}{\partial \boldsymbol{J}}\frac{\partial \boldsymbol{J}}{\partial \nu_i} \tag{5}$$

where $\boldsymbol{J}$ is the current density. Moreover, the second term of (4) is given as

$$\frac{\partial \boldsymbol{r}}{\partial \boldsymbol{A}} = \boldsymbol{H} + \frac{\partial \boldsymbol{H}}{\partial \nu_i}\frac{\partial \nu_i}{\partial \boldsymbol{B}^2}\frac{\partial \boldsymbol{B}^2}{\partial \boldsymbol{A}}\boldsymbol{A} - \frac{\partial \boldsymbol{G}}{\partial \boldsymbol{J}}\frac{\partial \boldsymbol{J}}{\partial \boldsymbol{B}^2}\frac{\partial \boldsymbol{B}^2}{\partial \boldsymbol{A}} \tag{6}$$

where $\boldsymbol{B}$ is the flux density. Since $\boldsymbol{J}$ is not a function of ν_i and $\boldsymbol{B}^2$ in the problem shown in Section III, the second term of (5) and the third term of (6) is zero. Substituting (5) and (6) into (4)

$$\frac{\mathrm{d}\boldsymbol{r}}{\mathrm{d}\nu_i} = \frac{\partial \boldsymbol{H}}{\partial \nu_i}\boldsymbol{A} + (\boldsymbol{H} + \Delta\boldsymbol{H})\frac{\partial \boldsymbol{A}}{\partial \nu_i} = 0. \tag{7}$$

The nonlinear term $\Delta\boldsymbol{H}$ of the $\boldsymbol{H}$ matrix taking account of the nonlinear magnetic property in the Newton–Raphson method (NR method) is given by

$$\Delta\boldsymbol{H} \equiv \frac{\partial \boldsymbol{H}}{\partial \nu_i}\frac{\partial \nu_i}{\partial \boldsymbol{B}^2}\frac{\partial \boldsymbol{B}^2}{\partial \boldsymbol{A}}\boldsymbol{A}. \tag{8}$$

As W is not a function of ν_i in the problem discussed here, and by substituting (7) into (1), (9) can be obtained

$$\frac{\mathrm{d}W}{\mathrm{d}\nu_i} = -\left\{\frac{\partial W}{\partial \boldsymbol{A}}^T(\boldsymbol{H} + \Delta\boldsymbol{H})^{-1}\right\}\frac{\partial \boldsymbol{H}}{\partial \nu_i}\boldsymbol{A}. \tag{9}$$

In order to avoid the calculation of the inverse of $(\boldsymbol{H}\Delta\boldsymbol{H})$, an adjoint vector $\boldsymbol{\lambda}$ is introduced [3]. The adjoint equation is given by

$$(\boldsymbol{H} + \Delta\boldsymbol{H})^T\lambda = \frac{\partial W}{\partial \boldsymbol{A}} \tag{10}$$

Digital Object Identifier 10.1109/TMAG.2006.871422

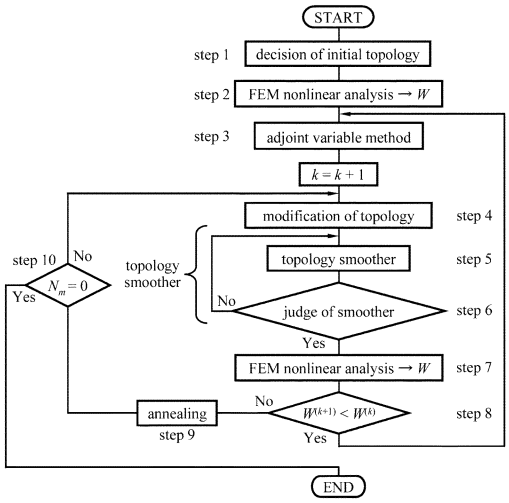

Fig. 1. Flowchart of ON/OFF method.

where $\boldsymbol{\lambda}$ is obtained by solving (10), and $\mathrm{d}W\mathrm{d}\nu_i$ is calculated by substituting $\boldsymbol{\lambda}$ into (11)

$$\frac{\mathrm{d}W}{\mathrm{d}\nu_i} = -\boldsymbol{\lambda}^T \frac{\partial \boldsymbol{H}}{\partial \nu_i}\boldsymbol{A}. \tag{11}$$

B. ON/OFF Topology Optimization Method

The ON/OFF method based on the sensitivity analysis is applied in order to obtain an actual topology within a shorter CPU. The edge-based 3-D FEM using brick elements is applied in the magnetic-field calculation.

The flowchart of the ON/OFF method is shown in Fig. 1.

Step 3) **adjont variable method**
Solving the adjoint (10) of the obtained topology, the sensitivity is calculated by (11).

Step 4) **modification of topology**
If the sensitivity $\mathrm{d}W/\mathrm{d}\nu_i$ is negative, the permeability in an element i should be increased. Then, the magnetic material is located in the element i. On the other hand, if the sensitivity $\mathrm{d}W/\mathrm{d}\nu_i$ is positive, the permeability in the element i should be decreased. Then, the air is allocated in the element i.

Step 5) **topology smoother**
Some caves may often be generated in an obtained magnetic circuit. Once such a domain is generated in subsequent repetitive steps, an uneven shape may arise, then such a shape cannot be adapted. Therefore, the topology smoother shown in Section II-C is introduced in order to solve this problem.

Step 6) **judge of smoother**
The smoothing of topology is executed until no material is changed by the smoother.

Step 9) **annealing**
If the objective function is not improved, the number of changeable elements is decreased. [2].

C. Topology Smoother

If the material of the evaluated element satisfies the following condition, the material of the element is changed.

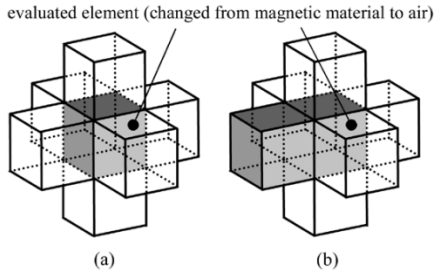

Fig. 2. Element changed from the magnetic material to air (cut step). (a) All neighboring elements are air. (b) One neighboring element is the magnetic material.

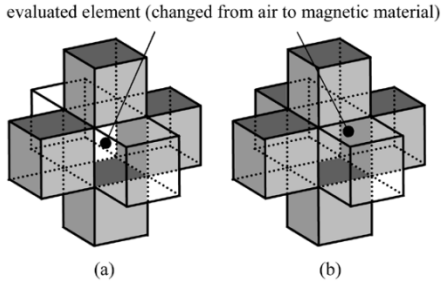

Fig. 3. Element changed from air to magnetic material (attached step). (a) Four neighboring elements are magnetic material. (b) Five neighboring elements are magnetic material.

1) **cut step**
If the material of the evaluated element is of a magnetic material, and those of all surrounding elements are air, or the material of one adjacent element is magnetic material and those of all other elements are air, the material of the evaluated element is changed from the magnetic material to the air as shown in Fig. 2. This operation can protect from the convex shape, in addition, to avoid the magnetic material floats in the air.

2) **attached step**
If the material of the evaluated element is in the air, and those of four or five neighboring elements are magnetic material, the material of the evaluated element is changed from the air to the magnetic material as shown in Fig. 3. This operation can protect from the concave shape.

The operations of (a) cut step and (b) attached step are repeated until the changing element disappears.

D. Method for Reducing CPU Time

In the 3-D topology optimization, the CPU time reduction technique of the FEM calculation is a very important item. The NR method with the line-search technique [4] is applied in the nonlinear analysis.

Furthermore, the matrix profile is minimized by using the Reverse Cuthill–McKee algorithm [6] in order to improve the convergence characteristic of the Incomplete Cholesky Conjugate Gradient (ICCG) solver.

III. Analyzed Model and Objective Function

Fig. 4 shows the analyzed model ($x - y$ plane) of the SPT head. The ampere-turns of the coil are 0.2AT. The FEM model is shown in Fig. 5. The underlayer is intentionally omitted to show the design domain and surrounding region clearly. The

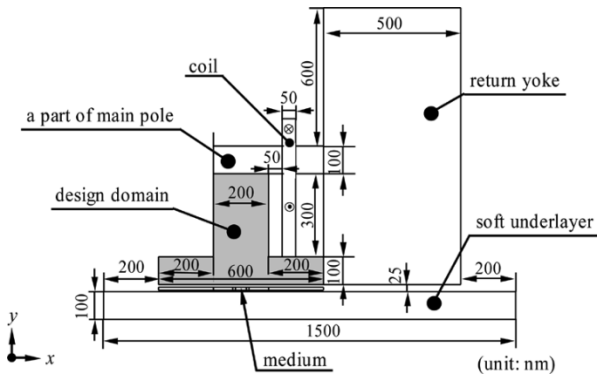

Fig. 4. Analyzed model (x-y plane).

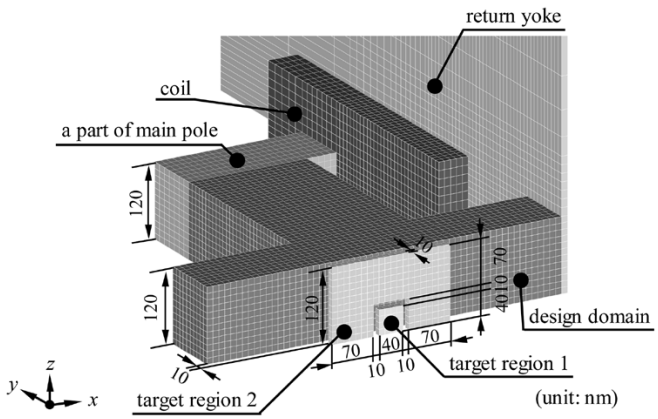

Fig. 5. FEM model of the SPT head (upper half region).

FEM model is composed of edge-based brick elements of the first order (217 152 elements, 229 416 nodes, 675 785 edges, 627 521 unknowns). FeCoAlO (saturated magnetization: 2.4 T) [2] is adopted as the magnetic material of the return yoke, the underlayer, a part of main pole, and the design domain corresponding to the yoke.

The design goal of the SPT head is to maximize the flux density (recording flux) in the target region 1 (on which a bit should be written), and to minimize the flux density (leakage flux) in the target region 2 (on which a bit should not be written simultaneously) in the medium. The functions W_1 and W_2 in the target regions 1 and 2 to be minimized are given as

$$W_1 = \int\int\int_{V_1} 1/B_y^2 \mathrm{d}V \tag{12}$$

$$W_2 = \int\int\int_{V_2} \left(B_x^2 + B_y^2 + B_z^2\right) \mathrm{d}V \tag{13}$$

where V_1 and V_2 are the volumes of target regions 1 and 2, and B_x, B_y and B_z are the x, y and z components of flux density. The objective function W is the linear combination of W_1 and W_2 given as

$$W = kW_1 + (1-k)W_2 \tag{14}$$

where $k (0 \leq k \leq 1)$ is the weighting coefficient.

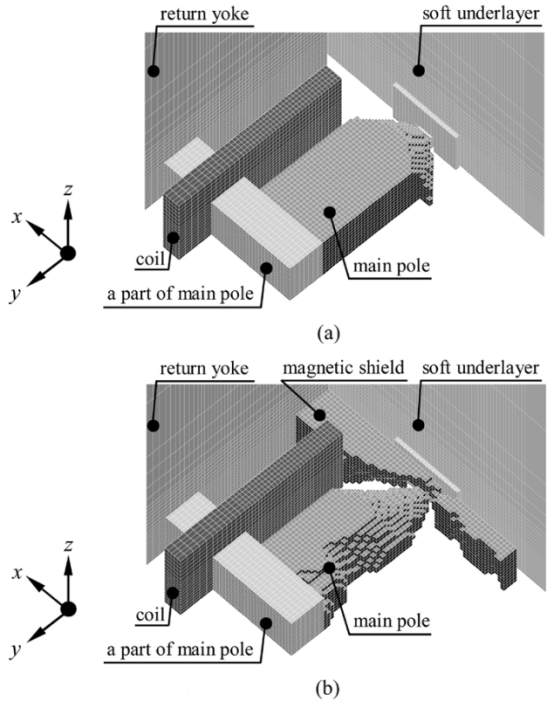

Fig. 6. Optimization process ($k = 0.5$). (a) First iteration ($W_1 = 1.06 \times 10^{-23}, W_2 = 7.44 \times 10^{-23}$). (b) Optimal topology (22nd iteration, $W_1 = 1.67 \times 10^{-23}, W_2 = 7.44 \times 10^{-24}$).

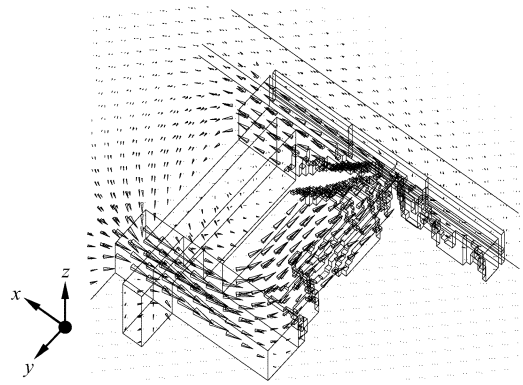

Fig. 7. Flux density vector ($k = 0.5$).

IV. Results and Discussion

A. Optimization Result

Fig. 6 shows the optimization process when $k = 0.5$. The initial material in the design domain is chosen as the air. An outline of the main pole is generated at the first iteration in order to maximize the recording flux. At the optimal topology (22nd iteration), the shape of the main pole is improved, and the magnetic shield is generated in order to prevent the leakage flux in the target region 2. The distribution of flux density vector is shown in Fig. 7. The main pole, which leads the flux efficiently in the target region 1, is obtained. The shield to reduce the leakage flux in the target region 2 is formed. Fig. 8 shows the flux distribution in the down track direction (x-axis) in the medium. Although the average flux density in the target region 2 is about 0.15 T, the flux density near the edge of the region is about 0.69 T. This means that the medium is magnetized near the edge of the region 2. The total number of FEM calculations is 288, and

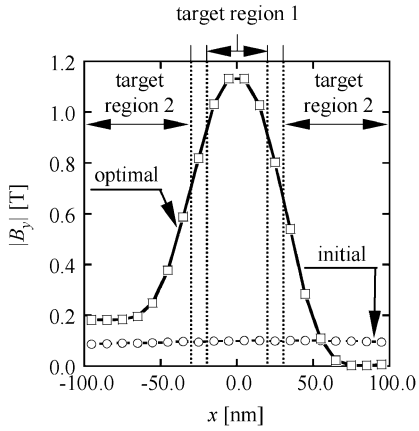

Fig. 8. Flux density in target regions 1 and 2 ($k = 0.5$).

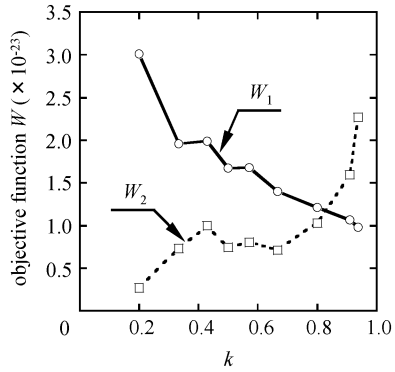

Fig. 9. Effect of k on values W_1 and W_2.

the CPU time is 81.6 h by using the PC (CPU: Pentium 4 Processor 3.2 GHz, random-access memory (RAM): 2.0 GB).

B. Effect of Weighting Coefficient

Fig. 9 shows the effect of k on the values of W_1 and W_2 at the optimal topology. When k is increased, W_1 is reduced and W_2 is increased. Fig. 10 shows the effect of k on the average value of the y component of flux density $|B_{y1\mathrm{ave}}|$ in the recorded region (target region 1) and $|B_{2\mathrm{ave}}|$ in the adjacent region (target region 2). The minimum value $|B_{y1\mathrm{min}}|$ in the target region 1 and the maximum value $|B_{2\mathrm{max}}|$ in the target region 2 are also shown. As $|B_{2\mathrm{max}}|$ exceeds 0.6 T when k is larger than 0.5, it seems that $k = 0.5$ is an acceptable maximum value. As the edge of region 2 may be magnetized as discussed in Fig. 8, an improved design of the head should be investigated. In order to minimize the leakage flux in the target region 2, the optimal design of the head having a smaller target region 2 should be carried out in the future.

V. Conclusion

The topology optimization of the SPT head is performed by using the ON/OFF method. The obtained results are summarized as follows.

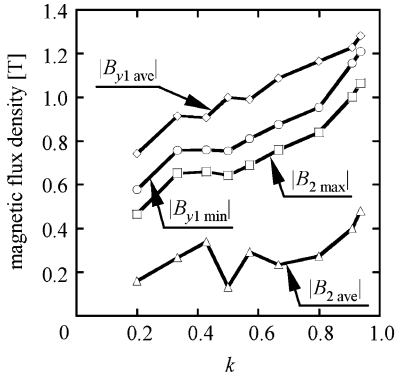

Fig. 10. Effect of k on flux densities in target regions 1 and 2.

1) The practical 3-D topology optimization method using the ON/OFF method combined with the topology smoother is proposed.
2) It is shown that the 3-D topology optimization of the SPT head, in which the main flux is increased and the leakage flux is decreased, is possible using the proposed method.
3) When the objective function is composed of more than two kinds of functions, the choice of the weighting coefficient is important in order to obtain a more desired result.

The introduction of the concept of the Pareto optimality is the future subject.

Acknowledgment

This work was supported by the Storage Research Consortium (SRC), Japan.

References

[1] C. H. Im, H. K. Jung, and Y. J. Kim, "Hybrid genetic algorithm for electromagnetic topology optimization," *IEEE Trans. Magn.*, vol. 39, no. 5, pp. 2163–2169, Sep. 2003.
[2] Y. Okamoto, M. Ohtake, and N. Takahashi, "Magnetic shield design of perpendicular magnetic recording head by using topology optimization technique," *IEEE Trans. Magn.*, vol. 41, no. 5, pp. 1788–1791, May 2005.
[3] J. Yoo, N. Kikuchi, and J. L. Volakis, "Structural optimization in magnetic devices by the homogenization design method," *IEEE Trans. Magn.*, vol. 36, no. 3, pp. 574–580, May 2000.
[4] K. Fujiwara, Y. Okamoto, A. Kameari, and A. Ahagon, "The Newton-Raphson method accelerated by using a line search—Comparison between energy functional and residual minimization—," *IEEE Trans. Magn.*, vol. 41, no. 5, pp. 1724–1727, May 2005.
[5] S. Gitosusastro, J. L. Coulomb, and J. C. Sabonnadiere, "Performance derivative calculations and optimization process," *IEEE Trans. Magn.*, vol. 25, no. 4, pp. 2834–2839, Jul. 1989.
[6] E. Cuthill and J. MacKee, "Reducing the bandwidth of sparse symmetric mtrices," in *Proc. ACM National Conf.*, San Francisco, CA, 1969.

Manuscript received June 20, 2005 (e-mail: norio@eplab.elec.okayama-u.ac.jp).